I&EC research
Industrial & Engineering Chemistry Research

Article

Cite This: Ind. Eng. Chem. Res. 2019, 58, 16934−16944

pubs.acs.org/IECR

Functional-Segment Activity Coefficient Equation of State: F-SAC-Phi

Luis F. Baladão, Paula B. Staudt, and Rafael de P. Soares*

Virtual Laboratory for Properties Prediction (LVPP), UFRGS, Department of Chemical Engineering, Federal University of Rio Grande do Sul, Rua Ramiro Barcelos, 2777, CEP 90035-007 Porto Alegre, RS, Brazil

ABSTRACT: COSMO-RS refinements and applications have been the focus of numerous works, mainly due to their great predictive capacity. However, these models do not directly include pressure effects. In this work, a methodology for the inclusion of pressure effects in the functional-segment activity coefficient model, F-SAC (a COSMO-based group-contribution method), is proposed. This is accomplished by the combination of F-SAC and lattice-fluid ideas by the inclusion of free volume in the form of holes, generating the F-SAC-Phi model. The computational cost when computing the pressure (given temperature, volume, and molar volume) with the proposed model is similar to the cost for computing activity coefficients with any COSMO-type implementation. For a given pressure, the computational cost increases since an iterative method is needed. The concept is tested for representative substances and mixtures, ranging from light gases to molecules with up to 10 carbons. The proposed model is able to correlate experimental data of saturation pressure and saturated liquid volume of pure substances with deviations of 1.7 and 1.1%, respectively. In the prediction of mixture vapor−liquid equilibria, the resulting model is superior to COSMO-SAC-Phi, SRK-MC (Soave−Redlich−Kwong with the Mathias−Copeman α-function) with the classic van der Waals mixing rule, and PSRK in almost all tested cases, from low pressures to over 100 bar.

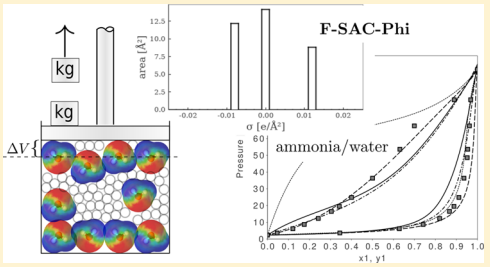

1. INTRODUCTION

Although COSMO-RS[1] models have exceptional theoretical characteristics and perform very well in qualitative, semi-quantitative, and solvent-screening tests, the precision required for engineering tasks, such as the optimization of separation systems, is usually beyond the current model resolution. In this sense, the F-SAC model[2,3] (which combines group contribution with the COSMO-RS theory) is an interesting alternative for the prediction of mixture behavior. This model is successfully applied to a variety of phase equilibria computations,[4] water−oil mutual solubilities,[5,6] multicompound systems,[7] and ionic liquids.[8]

However, these models describe only incompressible liquids, failing to describe the effects of pressure on thermodynamic properties and also with limited applicability to light gases. In the literature, there are some approaches that attempt to couple calculations of COSMO-type models with equations of state to model compressible phases. Lin[9] presented a study that deduced an equation of state based on the solvation theory of Ben-Naim.[10] Panayiotou et al.[11−13] developed an equation of state based on COSMO-RS. The authors calculated chemical potentials of interacting surfaces in terms of nonrandomness factors, generating the so-called NRCOSMO model. The authors removed the electrostatic contribution from COSMO-RS, keeping only the hydrogen-bond part to avoid inconsistencies in the ideal gas (IG) limit. The method was applied for some normal alkanes and polyethylene; later, the author also computed solvation/hydration properties.[11,13] In the work of Shimoyama and Iwai,[14] the authors introduced vacancies to the surface charge segments of the solvent molecule in the so-called COSMO-vac model. The resulting model was able to calculate activity coefficients in a supercritical phase. The solubilities of 16 pharmaceuticals in supercritical CO_2 predicted by COSMO-vac deviated from experimental values, on average, by less than unity, on the logarithmic scale. However, the method only computes infinite dilution activity coefficients of a solute in a fluid and cannot be seen as a complete equation of state. No expression for fugacity coefficients is demonstrated.

Costa et al.[15,16] developed the equation of state called σ-MTC, an extension of the Mattedi−Tavares−Castier equation,[17] which combines the sigma profile from COSMO computations with the generalized van der Waals theory. The estimated parameters were the lattice cell molar volume of component i (v_i^*) and the nonelectrostatic interaction energy parameters ($\langle C_{0,NE}\rangle_i$ and $\langle C_{1,NE}\rangle_i$).

Another recent approach investigated in the literature includes the use of the COSMO-SAC[18] model in mixing rules for cubic equations of state; for instance, combining SCMR[19] (self-consistent mixing rule) with COSMO-SAC to get a cubic equation of state with a strong predictive capacity. Wang et al.[20] also used SCMR when modeling polymer/gas mixtures based on COSMO-SAC. The authors proposed a modified version mSCMR and concluded that it is superior to the Wong−Sandler[21] and MHV1[22] mixing rules for the cases studied.

Received: April 22, 2019
Revised: August 5, 2019
Accepted: August 9, 2019
Published: August 9, 2019

DOI: 10.1021/acs.iecr.9b02190
Ind. Eng. Chem. Res. 2019, 58, 16934−16944

More recently another method for the inclusion of pressure effects in COSMO-type activity coefficient models was proposed, called COSMO-SAC-Phi or CSP[23] for short. The method is similar to COSMO-vac or NRCOSMO, consisting in creating a pseudo-mixture of molecules and holes (representing free volume). The ideal gas limit is recovered by subtracting the ideally screened state reference. This allows a seamless extension of any COSMO-based method to include pressure effects and compute fugacity coefficients of pure fluids and mixtures. Different from NRCOSMO, both electrostatic and hydrogen-bond contributions are considered and computed with standard COSMO-SAC equations. This method successfully predicted vapor−liquid equilibrium (VLE) and liquid−liquid equilibrium phase equilibria data with good accuracy for a variety of systems. However, due to its highly predictive nature, there is little room for improvement (e.g., correlation) of mixture data when the predictions deviate from experimental observations.

Thus, the objective of this work is to use the COSMO-SAC-Phi method with the F-SAC group-contribution method rather than COSMO-SAC. This will reduce the prediction power, but will provide more correlative power. The resulting model is called F-SAC-Phi or simply FSP.

2. COSMO-SAC-PHI AND F-SAC-PHI MODELS

In this work, the COSMO-SAC-Phi method is combined with F-SAC instead of COSMO-SAC, resulting in the F-SAC-Phi model. The main difference between F-SAC-Phi and COSMO-SAC-Phi or COSMO-RS models is that the latter ones rely on molecular properties determined by quantum chemical packages, whereas the F-SAC-Phi model (as well as pure F-SAC and other group-contribution methods) relies on fitted molecular properties.[2] In COSMO-SAC-Phi, the volume of the molecules is constant, and the effects of pressure and expansion are represented by the presence of holes (free volume). The formulation of the model is similar to the one in the works of Carnahan and Starling,[24] Chen and Kreglewski,[25] and Christoforakos and Franck,[26] with the pressure given by the sum of two contributions

$$P = P_R + P_A \tag{1}$$

where P_R is the pressure due to the repulsion forces and P_A is the contribution of pressure due to the forces of attraction.

Thus, this model can also be seen as a perturbation model,[27] with a simple fluid as reference (P_R) and a COSMO-based perturbation term (P_A).

2.1. Attractive Contribution by a Pseudo-Mixture. In the COSMO-SAC-Phi[23] method, the attractive contribution is computed by means of a pseudo-mixture, as shown in Figure 1.

Note that in the scheme of Figure 1, a pressure variation is possible as a function of volume. The real mixture is described by the mole amount vector $\mathbf{n} = [n_1, n_2, ..., n_i, ..., n_N]$. The pseudo-mixture is described by the combination of the real mole amount vector and the amount of holes $\tilde{\mathbf{n}} = [\mathbf{n}, n_h]$. This way the mixture volume is given simply by

$$V = \sum_i n_i b_i + n_h b_h \tag{2}$$

where b_i is the molar covolume of species i and b_h is the molar covolume of a hole.

Following Figure 1, pressure−volume relations are possible by the inclusion or removal of holes. This feature is not present in COSMO-RS, COSMO-SAC, or original F-SAC. For a given

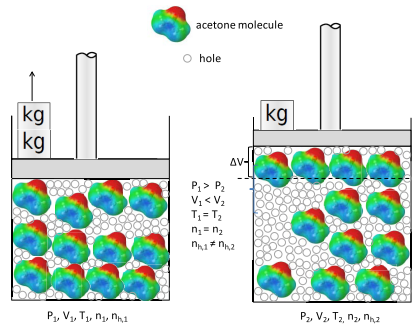

Figure 1. Schematic diagram for the COSMO-SAC-Phi model; holes of fixed volume are introduced when the pressure is reduced.

total volume and mole amount vector, eq 2 can be used to compute the hole mole amount

$$n_h = \frac{1}{b_h}\left(V - \sum_i n_i b_i\right) \tag{3}$$

For the calculation of attractive pressure P_A, a classic thermodynamic relation is used

$$P_A = -\left(\frac{\partial A_A^r}{\partial V}\right)_{T,\mathbf{n}} \tag{4}$$

where A_A^r is the residual Helmholtz energy of the attractive contribution. To simplify the notation, we will drop subscript A from here forward.

Considering the pseudo-mixture scheme of Figure 1, we can derive the required Helmholtz derivative by

$$\left(\frac{\partial A^r}{\partial V}\right)_{T,\mathbf{n}} = \left(\frac{\partial \tilde{A}^r}{\partial n_h}\right)_{T,\mathbf{n}}\left(\frac{\partial n_h}{\partial V}\right)_{T,\mathbf{n}} \tag{5}$$

where $\tilde{A}^r$ is the residual Helmholtz energy of the pseudo-mixture, and the last term of eq 5 is directly obtained by deriving eq 3

$$\left(\frac{\partial n_h}{\partial V}\right)_{T,\mathbf{n}} = \frac{1}{b_h} \tag{6}$$

Finally, we can define the residual chemical potential of the holes in the pseudo-mixture as

$$\tilde{\mu}_h^r \equiv \left(\frac{\partial \tilde{A}^r}{\partial n_h}\right)_{T,n_{j\neq h}} = \left(\frac{\partial \tilde{A}^r}{\partial n_h}\right)_{T,\mathbf{n}} \tag{7}$$

leading to an elegant result

$$P_A = -\left(\frac{\partial A^r}{\partial V}\right)_{T,\mathbf{n}} = -\frac{\tilde{\mu}_h^r}{b_h} \tag{8}$$

where $\tilde{\mu}_h^r$ is the hole residual chemical potential in the pseudo-mixture. The chemical potential of holes, $\tilde{\mu}_h$ (not residual), in the pseudo-mixture and the chemical potential of other components, $\tilde{\mu}_i$, are computed as usual with models such as COSMO-RS, COSMO-SAC, or F-SAC.

To obtain the residual version of these chemical potentials, the COSMO-SAC-Phi method consists in the following. Considering COSMO-SAC notation, we discretize a molecule surface into several segments, and the activity coefficient of a segment Γ_m is given by

DOI: 10.1021/acs.iecr.9b02190
Ind. Eng. Chem. Res. 2019, 58, 16934−16944

$$\ln \Gamma_m = -\ln\left\{\sum_n p_n \Gamma_n \exp\left[\frac{-\Delta W_{m,n}}{RT}\right]\right\} \tag{9}$$

where $\Delta W_{m,n}$ is the interaction energy between segments m and n, and p_n is the probability of finding segment n. In COSMO-SAC-Phi, both holes and molecules are always considered in eq 9. As stated by Lin and Sandler,[18] the logarithm of the activity coefficient of a segment $\ln \Gamma_m$ is actually a difference in chemical potentials. More precisely, $\ln \Gamma_m$ is the difference in chemical potential between the segment inserted into the actual mixture with respect to the segment inserted into a fluid of identical neutral segments.

To compute the residual contribution, and then respect the ideal gas limit, the neutral segment fluid reference should be replaced by the usual reference of an ideal gas (IG). This step is necessary because any computation with a COSMO-based model has an implicit reference state of a molecule surrounded by a perfect conductor, which is not an ideal gas (see, for instance, the so-called ideally screened state and eq 13 of ref 28). In the COSMO-SAC-Phi model, the ideal gas limit is recovered by the following subtraction

$$\ln \Gamma_m^{\mathrm{r}} = \ln \Gamma_m - \ln \Gamma_m^{\mathrm{IG}} \tag{10}$$

where $\ln \Gamma_{\mathrm{m}}^{\mathrm{IG}}$ is the chemical potential of the segment in an ideal gas, and $\ln \Gamma_{\mathrm{m}}^{\mathrm{r}}$ becomes the residual chemical potential of segment m.

The use of eq 10 is probably the major difference between COSMO-SAC-Phi and NRCOSMO.[11] In the latter model, the authors removed the electrostatic contribution of COSMO-RS, keeping only the hydrogen-bond part to avoid inconsistencies in the IG limit. In COSMO-SAC-Phi, the electrostatic contributions are not removed, and the IG reference state is actually recovered by eq 10.

The chemical potential of the segment in an ideal gas, $\ln \Gamma_{\mathrm{m}}^{\mathrm{IG}}$, can be calculated with eq 9 evaluated at the infinite molar volume limit, at the same temperature, by simply making the pseudo-mixture mole amount vector as

$$\tilde{\mathbf{n}}^{\mathrm{IG}} = [\mathbf{n} = \mathbf{0},\ n_{\mathrm{h}} = 1] = [0, 0, ..., 1] \tag{11}$$

Finally, with the residual chemical potential of each segment, we can calculate the residual chemical potential of a given compound (or hole) by summing its segments

$$\tilde{\mu}_i^{\mathrm{r}} = RT \sum_{m \in i} \left(\frac{Q_m}{a_{\mathrm{eff}}}\right) \ln \Gamma_m^{\mathrm{r}} \tag{12}$$

$$\tilde{\mu}_{\mathrm{h}}^{\mathrm{r}} = RT \sum_{m \in \mathrm{h}} \left(\frac{Q_m}{a_{\mathrm{eff}}}\right) \ln \Gamma_m^{\mathrm{r}} \tag{13}$$

where $a_{\mathrm{eff}} = \pi r_{\mathrm{av}}^2$ is the standard surface area segment and r_{av} is the averaging radius; Q_m is the surface area of segment m.

2.2. Fugacity Coefficients. Fugacity coefficients can be computed by[29]

$$\ln \hat{\phi}_i = \frac{1}{RT}\left(\frac{\partial A^{\mathrm{r}}}{\partial n_i}\right)_{T,V,n_j} - \ln Z \tag{14}$$

where $Z \equiv PV/NRT$ is the compressibility factor.

Since we consider that interactions come from a sum of repulsive and attractive forces, residual Helmholtz energy is $A^{\mathrm{r}} = A_{\mathrm{R}}^{\mathrm{r}} + A_{\mathrm{A}}^{\mathrm{r}}$. Again, we describe only the attractive contribution in this section and drop the subscript to simplify the notation.

To evaluate the Helmholtz partial derivative of eq 14 for a COSMO-SAC-Phi[23] pseudo-mixture, an increase in the amount n_i should cost a reduction in the amount of holes n_{h} to keep a constant total volume V. This is illustrated in Figure 2 and can be transcribed to

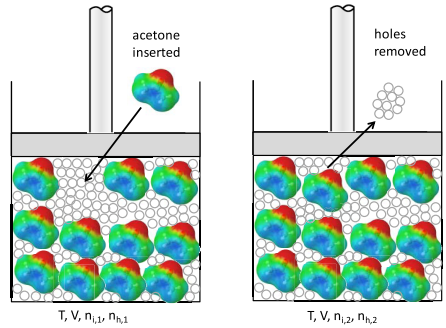

Figure 2. COSMO-SAC-Phi illustration of a system of constant total volume V: to introduce a new molecule, holes have to be removed.

$$\left(\frac{\partial A^{\mathrm{r}}}{\partial n_i}\right)_{T,V,n_j} = \left(\frac{\partial \tilde{A}^{\mathrm{r}}}{\partial n_i}\right)_{T,V,n_j,n_{\mathrm{h}}} + \left(\frac{\partial \tilde{A}^{\mathrm{r}}}{\partial n_{\mathrm{h}}}\right)_{T,V,\mathbf{n}} \left(\frac{\partial n_{\mathrm{h}}}{\partial n_i}\right)_{T,V,n_j} \tag{15}$$

where the last term on the right-hand side is obtained by deriving eq 3 (with constant b_{h})

$$\left(\frac{\partial n_{\mathrm{h}}}{\partial n_i}\right)_{T,V,n_j} = -\frac{b_i}{b_{\mathrm{h}}} \tag{16}$$

Combining eqs 15 and 16 with the chemical potential in eq 7, we obtain

$$\left(\frac{\partial A^{\mathrm{r}}}{\partial n_i}\right)_{T,V,n_j} = \tilde{\mu}_i^{\mathrm{r}} - \tilde{\mu}_{\mathrm{h}}^{\mathrm{r}} \frac{b_i}{b_{\mathrm{h}}} \tag{17}$$

Equation 17 can be applied to obtain fugacity coefficients of pure substances and fugacity coefficients of substances in mixtures. A detailed flowchart of all necessary steps for these computations is provided in the original work.[23]

If the hole volume, b_{h} (representing free volume), is not the same for every compound in the mixture, a mixing rule is used

$$b_{\mathrm{h}} = \sum_i \frac{n_i}{N} b_{\mathrm{h},i} \tag{18}$$

where $N = \sum_i n_i$ and $b_{\mathrm{h},i}$ is the hole volume for species i. Finally, the expression for the Helmholtz partial derivative of eq 14 would be

$$\left(\frac{\partial A^{\mathrm{r}}}{\partial n_i}\right)_{T,V,n_j} = \tilde{\mu}_i^{\mathrm{r}} - \tilde{\mu}_{\mathrm{h}}^{\mathrm{r}}\left(\frac{b_i}{b_{\mathrm{h}}} + \frac{n_{\mathrm{h}}}{N}(b_{\mathrm{h},i}/b_{\mathrm{h}} - 1)\right) \tag{19}$$

2.3. Repulsive Forces. Using the same approximation considered in the COSMO-SAC-Phi method, in the present work, a simple hard-sphere model was chosen to represent repulsive forces (reference fluid)

$$P_{\mathrm{R}} = \frac{NRT}{V - \sum_i n_i b_i} \tag{20}$$

DOI: 10.1021/acs.iecr.9b02190
Ind. Eng. Chem. Res. 2019, 58, 16934−16944

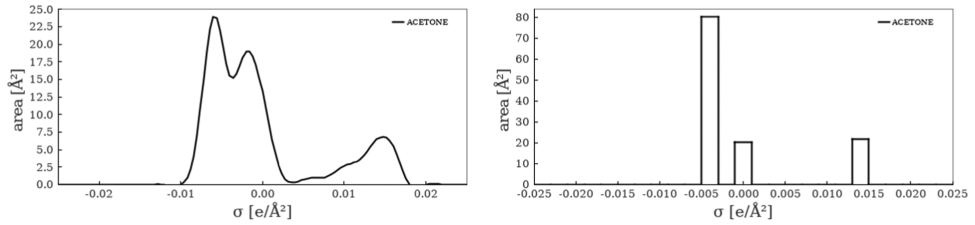

(a) COSMO-SAC (b) F-SAC

Figure 3. Comparison for the σ-profile of acetone for (a) COSMO-SAC[33] and (b) F-SAC.[2]

where $N = \sum_i n_i$, R is the universal gas constant, T is the temperature, and b_i is the hard-sphere volume of species i.

The hole amount, n_h, and its molar volume, b_h, should not be included in the summation of eq 20. It should be noted that this equation represents a crude simplification, and it is actually responsible for the so-called combinatorial contribution in the CSP model. Thus, more sophisticated representations, such as the Carnahan and Starling[30] or the more recent developments present in SAFT models,[31,32] may be used in future studies.

2.4. F-SAC-Phi Model. In the F-SAC model, the COSMO-RS theory of contacting surfaces is used. However, in the F-SAC model, each molecule is fragmented into functional groups, and each group has its own empirically calibrated σ-profile

$$p_k(\sigma)Q_k = \{(\sigma_k^-, Q_k^-); (0, Q_k^0); (\sigma_k^+, Q_k^+)\} \tag{21}$$

where the σ-profile of each functional group is represented by three empirical parameters: Q_k^-, Q_k^+, and σ_k^+. Q_k^+ represents the functional group area of the positive segment, Q_k^- is the functional group area of the negative segment, and σ_k^+ is the charge density of the positive segment. With these definitions, the neutral area Q_k^0 is given by the remaining area of the group surface area: $Q_k^0 = Q_k - Q_k^+ - Q_k^-$; and by a charge balance to keep each group neutral, the group negative charge density can be computed as $\sigma_k^- = \frac{\sigma_k^+ Q_k^+}{Q_k^-}$.

Finally, the σ-profile of a molecule is given by the sum of the σ-profiles of its constituent functional groups

$$p_i(\sigma)q_i = \sum_k \nu_k^{(i)} p_k(\sigma)Q_k \tag{22}$$

This discrete F-SAC σ-profile, in contrast to the usually continuous representation in COSMO-SAC or COSMO-RS, is shown in Figure 3.

Using the σ-profiles of compounds in the mixture, the proposed F-SAC-Phi model computes the fugacity coefficients, as explained in the previous section, based on the following pairwise surface contact energy[34]

$$\Delta W_{m,n} = \frac{\alpha'(\sigma_m + \sigma_n)^2}{2} + \frac{E_{m,n}^{HB}}{2} + \frac{E_{m,n}^{Disp}}{2} \tag{23}$$

where α' is the constant for the misfit energy, equal to 35 750 kJ Å^4/(mol e^2); σ_m and σ_n are the apparent surface charge densities of segments m and n (σ-profile); $E_{m,n}^{HB}$ and $E_{m,n}^{Disp}$ are the terms that take into account hydrogen bonds and dispersion between segments m and n, respectively.

In the F-SAC model, the HB term is a binary parameter[3] (for every functional group pair of HB donor and acceptor) to be fitted with mixture experimental data. The dispersion contribution was computed by the following simple combining rule

$$E_{m,n}^{Disp} = -\sqrt{\delta_m \delta_n} \tag{24}$$

where the segment dispersions, δ_m, are temperature-dependent, with a decay inspired by the one used in PC-SAFT models for the temperature-dependent segment diameters[31]

$$\delta_m = \delta_m^0(1 - \exp(-\delta_m^T/T)) \tag{25}$$

where δ_m^0 and δ_m^T were assumed to be per functional group k, with $m = k$ (adjusted in this work).

For the holes, the parameter, δ_h^0, was assumed to be zero and then the value of δ_h^T was irrelevant.

2.5. Parameter Estimation and Experimental Data. For every subgroup k, four parameters were estimated in the present work: volume (R_k and $b_{h,k}$) and dispersion parameters (δ_k^0 and δ_k^T). This was accomplished using pure compound saturation pressures (P^{sat}) and saturated liquid molar volume (v^l), collected from the literature with the aid of the NIST ThermoData Engine software.[35] The objective function (F_{obj}) for the optimization of the model parameters was as follows

$$F_{obj} = \frac{1}{NP}\sum_i^{NP} w\left(\frac{P_i^{sat,exp} - P_i^{sat,calc}}{P_i^{sat,exp}}\right)^2 + \left(\frac{v_i^{l,exp} - v_i^{l,calc}}{v_i^{l,exp}}\right)^2 \tag{26}$$

where NP is the number of experimental points; the "calc" superscript denotes the quantity calculated with the F-SAC-Phi, and $w = 10$ is a weighting factor,[4,36,37] so that priority is given to saturation pressure data.

For the saturation pressure calculations, a classical $\phi_i^l = \phi_i^v$ bubble point algorithm was used, and the fugacity coefficients were computed as previously described. After the bubble pressure algorithm converged, the saturated liquid volume was evaluated. To avoid the usual difficulties around the critical temperature T_c or at very low temperatures, only data in the interval $0.5\,T_c < T < 0.9T_c$ were considered, including around 20 experimental points for each substance.

The Nelder–Mead optimization method[38] was used to estimate the model parameters for each substance. First, the parameters for the linear hydrocarbon subgroups CH_3 and CH_2 were all adjusted using data of linear alkanes. After that, the other subgroup parameters were adjusted leaving the previously estimated parameters fixed.

All other F-SAC parameters, namely, Q_k (total area of subgroup k), Q_k^+ (area of the positive segment for subgroup k), Q_k^- (area of the negative segment), and σ_k^+ (positive segment surface charge density) as well as HB formation energies, were taken from previous works[2,3] and not optimized. For light gases unavailable in the original works (CH_4, CH_3–CH_3, N_2, H_2S, CO_2, NH_3, C_2H_4, and CH_3NH_2), the total area, Q_k, was taken directly from the COSMO cavity surface area available in the LVPP sigma-profile database[39] using the JCOSMO package developed by Gerber and Soares.[33,40] The electrostatic parameters (Q_k^+, Q_k^-, and σ_k^+) for the groups H_2 and N_2 were

DOI: 10.1021/acs.iecr.9b02190
Ind. Eng. Chem. Res. 2019, 58, 16934–16944

arbitrated as zero (nonpolar). For polar gases (CO_2, C_2H_4, and NH_3), the electrostatic parameters (Q_k^+, Q_k^-, and σ_k^+) were also adjusted in this work. For these cases, bubble pressure deviations for some VLE data were used along with the pure compound data to adjust simultaneously all needed pure compound parameters.

3. RESULTS AND DISCUSSION

A few representative functional groups were considered in this work as a proof of concept. The resulting parameters optimized with pure compound data, as described before, are listed in Tables 1 and 2. The average relative deviations per compound for saturation pressure and saturated liquid molar volume are given in Table 3

$$\mathrm{ARD}_P = \frac{1}{\mathrm{NP}} \sum_{k=1}^{\mathrm{NP}} \left| \frac{P_k^{\mathrm{sat}} - P_k^{\mathrm{sat,calc}}}{P_k^{\mathrm{sat}}} \right| \tag{27}$$

$$\mathrm{ARD}_v = \frac{1}{\mathrm{NP}} \sum_{k=1}^{\mathrm{NP}} \left| \frac{v_k^{\mathrm{l}} - v_k^{\mathrm{l,calc}}}{v_k^{\mathrm{l}}} \right| \tag{28}$$

Comparisons with COSMO-SAC-Phi[23] and with classical Soave−Redlich−Kwong equation of state with Mathias−Copeman α-function[41] (SRK-MC) are also included in Table 2, recalling that three additional parameters are needed for the α-function, taken from Horstmann et al.[41] Regarding volume comparisons, SRK-MC results with the volume translation method proposed by Péneloux et al.[42] based solely on critical data[41] are used (SRK-MC+VT), since large deviations (average of 13% with values larger than 39%) are observed without volume correction.

For molecules consisting of a single subgroup (e.g., $CHCl_3$), similar F-SAC-Phi and COSMO-SAC-Phi parameters were obtained. Regarding the hole (free volume) parameter, $b_{h,i}$, the average of all subgroups of the F-SAC-Phi model was 12.91 Å^3, similar to the COSMO-SAC-Phi average value of 14.03 Å^3.

In Figure 4, responses for pure compound saturation pressures of some representative molecules are shown. Even though the MC parameters used were adjusted using data from

Table 1. F-SAC-Phi Electrostatic Parameters Estimated in This Work for Polar Light Gases[a]

	electrostatic parameters		
group	Q_k^+ [Å^2]	Q_k^- [Å^2]	δ_k^+ [e/nm^2]
CO_2[b]	9.811	11.926	0.011
H_2S[c]	8.197	5.682	0.010
NH_3[d]	7.169	7.873	0.016

[a]For all other functional groups, electrostatic parameters were taken from refs 2 and 3. [b]Mixture data with methane, benzene, and acetone. [c]Mixture data with nitrogen, methane, benzene, and cyclohexane. [d]Mixture data with benzene and *n*-decane.

Table 2. Volume and Dispersion Parameters for the F-SAC-Phi Model Estimated in This Work

		volume		dispersion	
group	subgroup	R_k [Å^3]	$b_{h,k}$ [Å^3]	δ_k^0 [kcal/mol]	δ_k^T [10^2 K]
CH_2	CH_4	50.639	11.760	0.466	2.815
	CH_3	37.836	8.800	0.455	5.008
	CH_2	28.098	18.656	1.072	1.463
	CH	20.217	20.778	0.167	9.000
	CH_3−CH_3	74.024	13.355	0.618	3.387
	c-CH_2	25.918	14.636	0.657	4.309
CH_3COCH_3	CH_3COCH_3	101.800	13.691	0.710	3.686
	CH_3COCH_2	92.212	15.309	0.866	3.564
CH_3COOCH_3	CH_3COOCH_3	110.032	12.511	0.686	3.321
	CH_3COOCH_2	102.941	15.141	0.873	2.657
ACH	ACH	21.475	15.959	0.835	4.708
	AC	17.645	16.225	7.628	20.109
CH_3OCH_2	CH_3OCH_3	82.652	12.482	0.638	3.623
	CH_2OCH_2	66.436	18.128	1.127	1.620
C═C	CH_2═CH	50.479	15.780	0.584	3.907
	c-CH═CH	33.728	15.556	0.708	4.347
c-CH_2OCH_2	c-CH_2OCH_2	62.440	12.671	0.817	4.412
CH_3OH	CH_3OH	56.892	9.812	1.086	3.868
CH_2OH	CH_2OH	33.355	15.312	7.978	0.334
$CHCl_3$	$CHCl_3$	93.939	16.491	0.860	4.043
$N(CH_2)_3$	$N(CH_2)_3$	106.427	18.613	2.260	1.819
CCl_4	CCl_4	137.853	15.270	0.720	4.735
CO_2	CO_2	45.229	9.761	0.592	3.116
H_2	H_2	35.885	11.293	0.135	1.644
N_2	N_2	45.877	10.745	0.332	1.678
H_2S	H_2S	46.389	10.846	0.714	5.137
H_2O	H_2O	24.373	6.906	1.218	9.183
NH_3	NH_3	30.928	8.699	0.632	7.291
C_2H_4	C_2H_4	66.267	12.695	0.591	3.286
CH_3NH_2	CH_3NH_2	58.139	11.874	0.829	4.262

DOI: 10.1021/acs.iecr.9b02190
Ind. Eng. Chem. Res. 2019, 58, 16934−16944

Table 3. Deviations of Saturation Pressure and Saturated Liquid Volume Using the F-SAC-Phi Model, COSMO-SAC-Phi, and SRK-MC+VT

		F-SAC-Phi		COSMO-SAC-Phi		SRK-MC+VT	
family	compound	ARD_P %	ARD_V %	ARD_P %	ARD_v %	ARD_P %	ARD_v %
saturated	methane	1.9	0.8	1.8	1.2	1.5	3.2
hydrocarbon	ethane	1.6	0.7	1.5	1.0	0.2	3.1
	propane	2.7	2.4	1.3	1.3	0.4	4.0
	n-butane	2.1	0.9	0.5	0.7	0.3	3.2
	n-pentane	3.9	1.7	0.3	0.4	0.2	3.1
	2-methylpentane	10.9	1.8	2.5	2.8	1.9	1.2
	n-hexane	4.6	1.3	0.6	1.6	1.2	3.7
	n-octane	3.8	0.9	0.9	2.5	3.4	4.1
	n-decane	3.2	3.7	2.0	4.5	1.4	4.9
	cyclohexane	0.7	0.5	0.7	1.0	0.4	3.4
unsaturated	ethylene	1.7	0.6	1.3	0.5	0.7	2.7
hydrocarbon	1-butene	1.0	0.6	0.5	0.6	2.6	3.2
	1-hexene	2.8	1.6	1.8	2.3	1.8	5.3
	cyclohexene	1.1	6.5	1.3	0.7	8.4	18.2
aromatic	benzene	0.9	0.3	0.8	0.5	0.5	3.8
	toluene	1.2	1.9	1.2	1.1	0.9	4.0
ketone	acetone	1.0	0.4	0.7	0.6	1.2	5.7
	methyl ethyl ketone	0.7	0.0	0.6	1.0	1.6	1.0
ether	dimethyl ether	0.5	1.1	0.8	1.1	2.3	16.0
	diethyl ether	1.0	1.8	0.4	0.4	0.8	4.6
	tetrahydrofuran	1.3	1.5	1.5	0.9	1.1	4.6
ester	methyl acetate	0.6	0.1	0.5	0.5	2.6	4.4
	ethyl acetate	1.8	3.5	0.7	1.4	1.0	4.1
organic halide	chloroform	1.4	0.8	1.0	3.2	1.2	12.2
	carbon tetrachloride	0.8	0.6	0.8	1.1	0.9	3.6
alcohol	methanol	1.4	0.6	1.0	2.4	0.8	6.9
	ethanol	2.1	3.3	1.8	4.0	2.8	5.7
	n-butanol	4.1	3.5	1.4	5.1	2.0	5.0
	n-pentanol	2.6	2.5	2.3	2.2	3.8	3.5
amine	methylamine	1.1	1.7	1.5	4.2	1.9	17.9
	triethylamine	1.9	1.0	1.2	1.3	3.5	3.2
gases	nitrogen	2.2	0.9	1.8	1.0	1.9	3.3
	carbon dioxide	1.3	1.1	0.2	0.2	0.8	5.8
	hydrogen sulfide	2.9	1.1	1.6	0.9	1.2	5.3
other	ammonia	1.7	1.0	2.3	2.2	1.5	6.5
	water	1.5	0.2	0.9	0.8	0.6	9.0
average		1.7	1.1	1.1	1.1	1.2	4.1

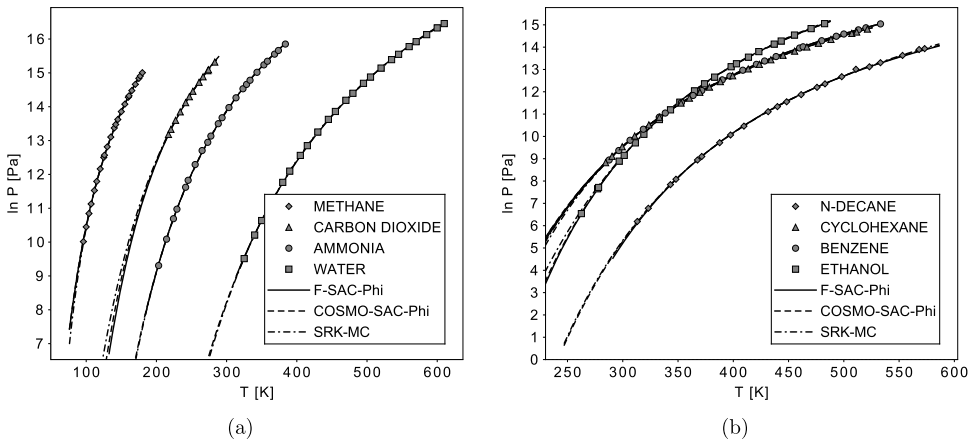

Figure 4. Saturation pressure for (a) small molecules and (b) larger molecules calculated with F-SAC-Phi, COSMO-SAC-Phi, and SRK-MC. Experimental data from TDE software with 20 experimental points for each substance.

different database software,[41] for most cases, the responses from F-SAC-Phi, COSMO-SAC-Phi, and SRK-MC are visually indistinguishable and in very good agreement with experimental data.

DOI: 10.1021/acs.iecr.9b02190
Ind. Eng. Chem. Res. 2019, 58, 16934−16944

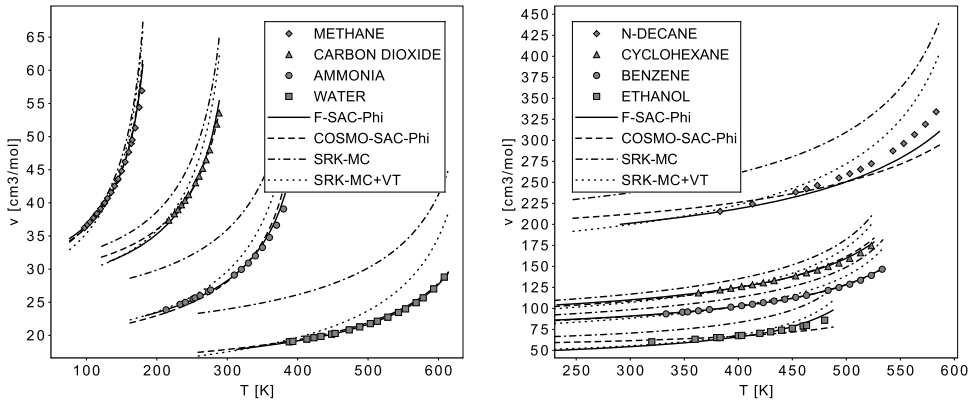

Figure 5. Saturated liquid molar volume for (a) small volumes and (b) larger volumes calculated with F-SAC-Phi, COSMO-SAC-Phi, SRK-MC, and SRK-MC+VT. Experimental data from TDE software with 20 experimental points for each substance.

Table 4. Relative Deviations of Bubble Pressures for F-SAC-Phi (FSP), COSMO-SAC-Phi (CSP), SRK-MC, and PSRK for Different Systems

			$AARD_P$ %			
system	ref	P (bar)	FSP	CSP	SRK-MC	PSRK
methyl acetate/1-hexene	43	0.6−1.0	3.1	2.3	10.1	1.1
methanol/water	44	0.2−0.8	4.9	3.2	37.3	1.0
acetone/cyclohexane	45	0.1−0.4	9.1	5.8	27.1	4.6
chloroform/benzene	46	0.3−0.7	0.9	1.6	4.8	0.7
chloroform/diethyl ether	47	0.2−0.7	4.2	3.4	21.5	7.3
chloroform/acetone	48	0.2−0.4	0.9	1.0	16.4	1.0
low pressure average			3.8	2.9	19.5	2.6
carbon dioxide/acetone	49	5−55	3.2	3.8	5.3	12.2
carbon dioxide/benzene	50	15−65	1.8	23.6	29.6	8.2
carbon dioxide/methanol	51	5−80	10.7	13.6	25.7	3.6
ammonia/*n*-butane	52	5−25	2.2	8.0	26.6	18.6
ammonia/benzene	53	1−4.5	2.7	9.4	41.2	12.6
ammonia/water	54	1−100	24.2	17.0	181.1	5.2
nitrogen/methane	55	3−35	4.3	3.5	5.8	1.5
methane/carbon dioxide	56	10−80	5.8	10.0	20.6	4.0
nitrogen/carbon dioxide	57	5−120	14.6	8.7	8.6	6.6
ethane/*n*-butane	58	12−38	4.0	4.3	2.3	3.1
ethane/*n*-pentane	59	1−50	6.4	8.6	4.6	8.4
ethane/*n*-decane	60	5−100	17.0	32.5	5.7	35.8
overall			8.1	11.9	29.8	10.0

In Figure 5, results for saturated liquid volume of some representative molecules are shown. As can be seen, the proposed method can correlate data very well for a variety of substances, in spite of the priority for correlation of vapor pressures in the objective function, eq 26.

When compared with SRK-MC results, much better agreement with experimental data is observed with the F-SAC-Phi and COSMO-SAC-Phi models. Poor results for the prediction of liquid volumes are well known for cubic equations of state. In Figure 5, results with the volume translation method proposed by Péneloux et al.[42] are also shown, referred to as SRK-MC+VT. In this work, the version based solely on critical data was considered.[41] This method indeed improved the results for cubic equations of state, but the proposed method's correlation was still superior.

When F-SAC-Phi is compared with COSMO-SAC-Phi, similar performance is observed for molecules consisting of a single functional group (e.g., methane, cyclohexane, and benzene). For molecules consisting of different subgroups (e.g., *n*-hexane, 1-hexene, and 2-methylpentane), the proposed method has shown some difficulties. This can be explained by the limitations of a group-contribution method, where different molecules need to be described by a single set of parameters, whereas in COSMO-SAC-Phi, there are per compound parameters. Furthermore, most parameters were taken from previous F-SAC works in this proof of concept (subgroup total area and electrostatic parameters). In future works, all parameters could be refined, probably leading to improved responses.

3.1. VLE Predictions. In this section, some vapor−liquid equilibrium (VLE) experimental data are compared with F-SAC-Phi, COSMO-SAC-Phi, SRK-MC+vdW, and PSRK predictions. SRK-MC+vdW corresponds to the SRK equation of state with the Mathias−Copeman α-function and the classical van der Waals mixing rule with no binary interaction parameters. PSRK also includes the MC α-function but relies on group-

DOI: 10.1021/acs.iecr.9b02190
Ind. Eng. Chem. Res. 2019, 58, 16934−16944

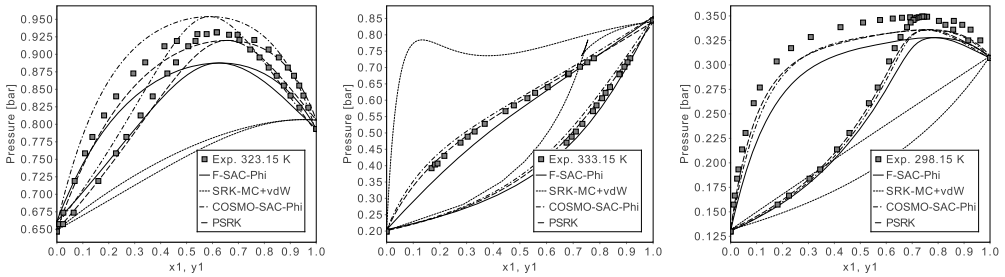

(a) methyl acetate/1-hexene[43] (b) methanol/water[44] (c) acetone/cyclohexane[45]

Figure 6. VLE predictions for F-SAC-Phi, COSMO-SAC-Phi, SRK-MC+vdW, and PSRK for low-pressure cases with positive deviations from the Raoult law.

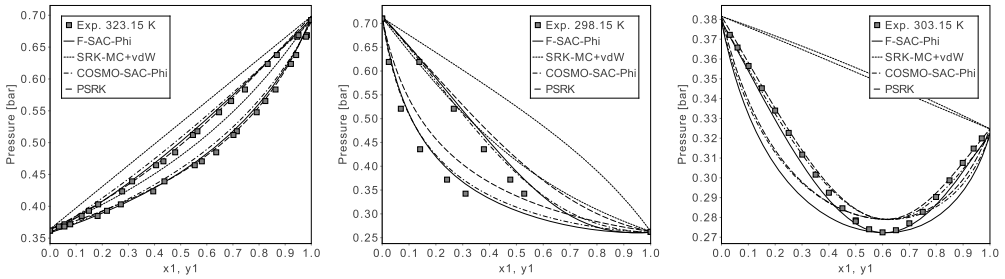

(a) chloroform/benzene[46] (b) chloroform/diethyl ether[47] (c) chloroform/acetone[48]

Figure 7. VLE predictions for F-SAC-Phi, COSMO-SAC-Phi, SRK-MC+vdW, and PSRK for low-pressure cases with negative deviations from the Raoult law.

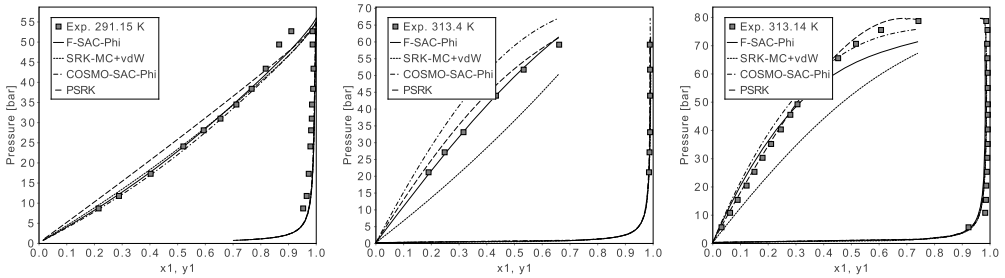

(a) carbon dioxide/acetone[49] (b) carbon dioxide/benzene[50] (c) carbon dioxide/methanol[51]

Figure 8. VLE predictions for F-SAC-Phi, COSMO-SAC-Phi, SRK-MC+vdW, and PSRK for carbon dioxide systems at high pressures.

contribution binary interaction parameters (UNIFAC-like) combined with SRK-MC by means of a specific mixing rule.[41] The intent is just to provide comparisons with a wide variety of models, ranging from the very simple SRK-MC+vdW to the PSRK method, which relies on large binary interaction parameter matrices. Results were produced based on the isofugacity criteria, $y_i\hat{\phi}_i^{v} = x_i\hat{\phi}_i^{l}$.

Results are listed in Table 4, including references for the experimental data. Only deviations of pressure are included, since not all experiments provide vapor phase composition data. Furthermore, deviations of pressure are usually correlated with deviations of vapor phase composition.

As can be seen in Table 4, the proposed FSP method provided results similar to CSP and PSRK for the low-pressure systems investigated. When high-pressure systems were also considered, the proposed method provided the smallest overall deviation.

Visual comparisons are available in Figures 6−11. In Figure 6, some low-pressure predictions are compared with experimental data for cases of positive deviations from the Raoult law. As can be seen, F-SAC-Phi responses are very similar to the ones obtained with COSMO-SAC-Phi. For all cases in this figure, F-SAC-Phi predictions are clearly superior to SRK-MC+vdW ones. The proposed method produced results very similar to PSRK and CSP for these cases, but they could be further improved if the original F-SAC parameters were refined specifically for use in the FSP method.

Predictions for some low-pressure cases with negative deviations from the Raoult law are shown in Figure 7. Again, F-SAC-Phi responses are very similar to the ones obtained with the COSMO-SAC-Phi model. For all cases in this figure, SRK-MC+vdW predicted nearly ideal behavior. This is a well-known deficiency of cubic equations of state with the classic mixing rule, unable to produce negative deviations without negative binary interaction parameters.[32] Results with the PSRK method are also in good agreement with the experimental data.

Predictions for systems with carbon dioxide are shown in Figure 8. For carbon dioxide/acetone, F-SAC-Phi, COSMO-SAC-Phi, and SRK-MC+vdW presented similar responses, in agreement with experimental data. PSRK performance was slightly worse for this case. For the case with benzene, much better agreement with experimental data is observed for the proposed model when compared with COSMO-SAC-Phi, SRK-

DOI: 10.1021/acs.iecr.9b02190
Ind. Eng. Chem. Res. 2019, 58, 16934−16944

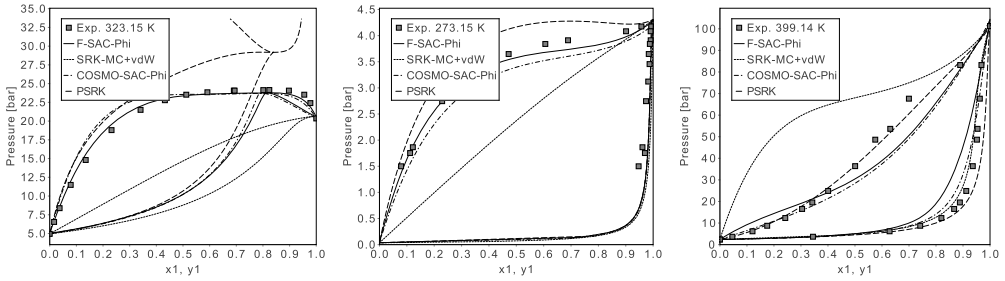

(a) ammonia/*n*-butane[52] (b) ammonia/benzene[53] (c) ammonia/water[54]

Figure 9. VLE predictions for F-SAC-Phi, COSMO-SAC-Phi, SRK-MC+vdW, and PSRK for ammonia systems at high pressures.

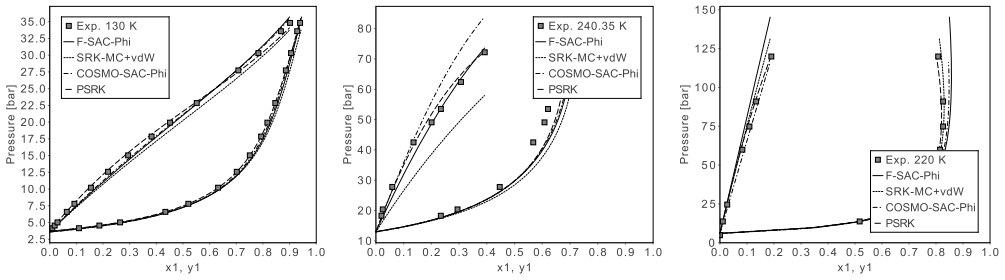

(a) nitrogen/methane[55] (b) methane/carbon dioxide[56] (c) nitrogen/carbon dioxide[57]

Figure 10. VLE predictions for F-SAC-Phi, COSMO-SAC-Phi, SRK-MC+vdW, and PSRK for light gas systems.

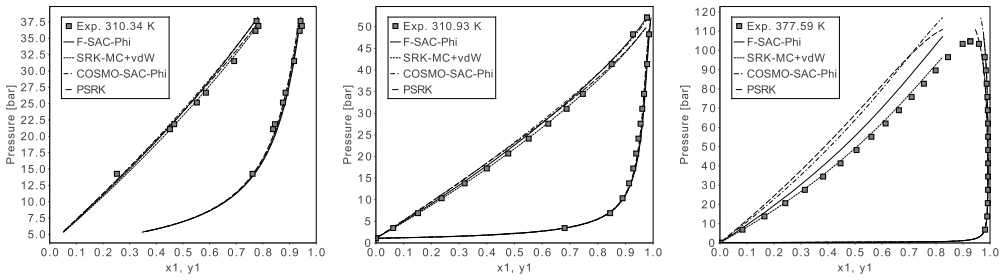

(a) ethane/*n*-butane[61] (b) ethane/*n*-pentane[59] (c) ethane/*n*-decane[60]

Figure 11. VLE predictions for F-SAC-Phi, COSMO-SAC-Phi, SRK-MC+vdW, and PSRK for ethane systems with different degrees of asymmetry.[61]

MC+vdW, and PSRK. For the mixture with methanol, all models provided similar performance, with a higher deviation for the simple cubic equation of state SRK-MC-vdW. This is one example where refined F-SAC parameters can show improved responses. Since there were no CO_2 parameters available in the original version, they were estimated also considering mixture data (see Table 1).

Predictions for systems with ammonia are shown in Figure 9. Again SRK-MC+vdW without binary interaction parameters could not predict the experimentally observed strong deviations. F-SAC-Phi, on the other hand, produced very good predictions for positive deviations as well as negative, with pressures up to 100 bar. COSMO-SAC-Phi and PSRK were superior to the proposed method only for the ammonia/water pair.

In Figure 10, VLE calculations for some light gas mixtures are shown. In these cases, good agreement with experimental data was observed for all models, with a slightly better performance for PSRK.

In Figure 11, ethane/hydrocarbon mixtures are used to verify how the proposed model handles asymmetric systems. As can be seen, the proposed model performance did not degrade as much as the system asymmetry becomes higher. This is an advantage over both PSRK and COSMO-SAC-Phi.

4. CONCLUSIONS

In this work, a method for the inclusion of pressure effects in the functional-segment activity coefficient model, F-SAC (group-contribution method), is proposed, allowing description of compressible phases and mixtures with light gases. The proposed modification consists of the direct combination of F-SAC and lattice-fluid ideas by the inclusion of holes, as suggested in the COSMO-SAC-Phi method. The resulting model was called F-SAC-Phi, or FSP for short.

In the proof of concept present in this work, a simple hard-sphere model was considered for the repulsion forces. Pure compound parameters were introduced accounting for dispersive interactions. The model was able to correlate well experimental saturation pressure and saturated liquid volume simultaneously with average deviations of 1.7 and 1.1%, respectively.

Mixtures ranging from light gases to molecules with up to 10 carbons were tested for low pressures as well as for pressures over 100 bar. Predictions of mixture vapor−liquid equilibrium (VLE) data with the proposed model performed similarly to COSMO-SAC-Phi, SRK-MC, and PSRK.

Future works can improve the repulsive contribution as well as the description of free volume. Responses could also be

DOI: 10.1021/acs.iecr.9b02190
Ind. Eng. Chem. Res. 2019, 58, 16934−16944

improved if the original F-SAC parameters were refined specifically to be used with F-SAC-Phi. Investigations around the critical point as well as critical compressibilities with F-SAC-Phi as well as COSMO-SAC-Phi are also to be pursued.

AUTHOR INFORMATION

Corresponding Author

*E-mail: rafael.pelegrini@ufrgs.br. Phone: +55 (51)3308-2852.

ORCID

Luis F. Baladão: 0000-0002-3904-4903

Paula B. Staudt: 0000-0002-5204-3980

Rafael de P. Soares: 0000-0002-0636-1363

Notes

The authors declare no competing financial interest.

ACKNOWLEDGMENTS

The authors would like to thank Brazilian agencies CAPES and CNPq (grant no. 304046/2016-7) that partially supported this research.

REFERENCES

(1) Klamt, A. Conductor-like Screening Model for Real Solvents: A New Approach to the Quantitative Calculation of Solvation Phenomena. *J. Phys. Chem. A* **1995**, *99*, 2224−2235.

(2) Soares, R. D. P.; Gerber, R. P. Functional-Segment Activity Coefficient Model. 1. Model Formulation. *Ind. Eng. Chem. Res.* **2013**, *52*, 11159−11171.

(3) Soares, R. d. P.; Gerber, R. P.; Possani, L. F. K.; Staudt, P. B. Functional-Segment Activity Coefficient Model. 2. Associating Mixtures. *Ind. Eng. Chem. Res.* **2013**, *52*, 11172−11181.

(4) Possani, L. F. K.; Flôres, G. B.; Staudt, P. B.; Soares, R. D. P. Simultaneous correlation of infinite dilution activity coefficient, vapor-liquid, and liquid-liquid equilibrium data with F-SAC. *Fluid Phase Equilib.* **2014**, *364*, 31−41.

(5) Possani, L.; Simões, R.; Staudt, P.; Soares, R. d. P. Mutual solubilities of hydrocarbon-water systems with F-SAC. *Fluid Phase Equilib.* **2014**, *384*, 122−133.

(6) Possani, L.; Staudt, P.; Soares, R. P. Prediction of water solubilities in hydrocarbons and oils using F-SAC coupled with SRK-EoS. *Fluid Phase Equilib.* **2016**, *427*, 394−405.

(7) Oliveira, N. C.; Soares, R. d. P. Correlation of vapor-liquid equilibrium data of amines in organic and aqueous mixtures with the F-SAC model. *Fluid Phase Equilib.* **2019**, *484*, 15−25.

(8) Schneider, R.; Gerber, R.; Soares, R. d. P. Extension of the F-SAC model to ionic liquids. *Fluid Phase Equilib.* **2018**, *477*, 87−97.

(9) Lin, S.-T. Thermodynamic equations of state from molecular solvation. *Fluid Phase Equilib.* **2006**, *245*, 185−192.

(10) Ben-Naim, A. *Solvation Thermodynamics*; Plenum Press, 1987.

(11) Panayiotou, C.; Tsivintzelis, I.; Aslanidou, D.; Hatzimanikatis, V. Solvation quantities from a COSMO-RS equation of state. *J. Chem. Thermodyn.* **2015**, *90*, 294−309.

(12) Panayiotou, C. Equation-of-State Models and Quantum Mechanics Calculations. *Ind. Eng. Chem. Res.* **2003**, *42*, 1495−1507.

(13) Panayiotou, C. Solvation thermodynamics and non-randomness. Part I: Self-solvation. *J. Chem. Eng. Data* **2010**, *55*, 5453−5464.

(14) Shimoyama, Y.; Iwai, Y. Development of activity coefficient model based on COSMO method for prediction of solubilities of solid solutes in supercritical carbon dioxide. *J. Supercrit. Fluids* **2009**, *50*, 210−217.

(15) Costa, C. T. O. G.; Tavares, F. W.; Secchi, A. R. Equation of state based on the hole-lattice theory and surface-charge density (COSMO): Part A - Pure compounds. *Fluid Phase Equilib.* **2016**, *409*, 472−481.

(16) Costa, C. T. O. G.; Tavares, F. W.; Secchi, A. R. Equation of state based on the hole-lattice theory and surface-charge density (COSMO): Part B - Vapor-liquid equilibrium for mixtures. *Fluid Phase Equilib.* **2016**, *419*, 1−10.

(17) Mattedi, S.; Tavares, F. W.; Castier, M. Group contribution equation of state based on the lattice fluid theory: Alkane-alkanol systems. *Fluid Phase Equilib.* **1998**, *142*, 33−54.

(18) Lin, S.-T.; Sandler, S. I. A Priori Phase Equilibrium Prediction from a Segment Contribution Solvation Model. *Ind. Eng. Chem. Res.* **2002**, *41*, 899−913.

(19) Staudt, P. B.; Soares, R. D. P. A self-consistent Gibbs excess mixing rule for cubic equations of state. *Fluid Phase Equilib.* **2012**, *334*, 76−88.

(20) Wang, L.-H.; Hsieh, C.-M.; Lin, S.-T. Prediction of Gas and Liquid Solubility in Organic Polymers Based on the PR+COSMOSAC Equation of State. *Ind. Eng. Chem. Res.* **2018**, *57*, 10628−10639.

(21) Wong, D. S. H.; Sandler, S. I. A theoretically correct mixing rule for cubic equations of state. *AIChE J.* **1992**, *38*, 671−680.

(22) Michelsen, M. L. A modified Huron-Vidal mixing rule for cubic equations of state. *Fluid Phase Equilib.* **1990**, *60*, 213−219.

(23) Soares, R. d. P.; Baladão, L. F.; Staudt, P. B. A pairwise surface contact equation of state: COSMO-SAC-Phi. *Fluid Phase Equilib.* **2019**, *488*, 13−26.

(24) Carnahan, N. F.; Starling, K. E. Intermolecular repulsions and the equation of state for fluids. *AIChE J.* **1972**, *18*, 1184−1189.

(25) Chen, S. S.; Kreglewski, A. Applications of the Augmented van der Waals Theory of Fluids.: I. Pure Fluids. *Ber. Bunsenges. Phys. Chem.* **1977**, *81*, 1048−1052.

(26) Christoforakos, M.; Franck, E. U. An Equation of State for Binary Fluid Mixtures to High Temperatures and High Pressures. *Ber. Bunsenges. Phys. Chem.* **1986**, *90*, 780−789.

(27) Kontogeorgis, G. M.; Voutsas, E. C.; Yakoumis, I. V.; Tassios, D. P. An Equation of State for Associating Fluids. *Ind. Eng. Chem. Res.* **1996**, *35*, 4310−4318.

(28) Klamt, A.; Jonas, V.; Bürger, T.; Lohrenz, J. C. W. Refinement and Parametrization of COSMO-RS. *J. Phys. Chem. A* **1998**, *102*, 5074−5085.

(29) Michelsen, M. L.; Mollerup, J. M. *Thermodynamic Models: Fundamentals & Computational Aspects*; Tie-Line Publications, 2007.

(30) Carnahan, N. F.; Starling, K. E. Equation of State for Nonattracting Rigid Spheres. *J. Chem. Phys.* **1969**, *51*, 635−636.

(31) Tihic, A.; Kontogeorgis, G. M.; Von Solms, N.; Michelsen, M. L.; Constantinou, L. A predictive group-contribution simplified PC-SAFT equation of state: Application to polymer systems. *Ind. Eng. Chem. Res.* **2008**, *47*, 5092−5101.

(32) Kontogeorgis, G. M.; Folas, G. K. *Thermodynamic Models for Industrial Applications: From Classical and Advanced Mixing Rules to Association Theorie*; John Wiley & Sons, Ltd, 2010; pp 1−692.

(33) Gerber, R. P.; Soares, R. D. P. Assessing the reliability of predictive activity coefficient models for molecules consisting of several functional groups. *Braz. J. Chem. Eng.* **2013**, *30*, 1−11.

(34) Flôres, G. B.; Staudt, P. B.; Soares, R. D. P. Including dispersive interactions in the F-SAC model. *Fluid Phase Equilib.* **2016**, *426*, 56−64.

(35) Frenkel, M.; Chirico, R. D.; Diky, V.; Yan, X.; Dong, Q.; Muzny, C. ThermoData Engine (TDE): Software Implementation of the Dynamic Data Evaluation Concept. *J. Chem. Inf. Model.* **2005**, *45*, 816−838.

(36) Sørensen, J. M.; Magnussen, T.; Rasmussen, P.; Fredenslund, A. Liquid-liquid equilibrium data: Their retrieval, correlation and prediction Part II: Correlation. *Fluid Phase Equilib.* **1979**, *3*, 47−82.

(37) Bender, N.; Cardozo, N. S. M.; de P. Soares, R. Avoiding binary interaction parameters in the GC-PC-SAFT model with a parametrization based in VLE and IDAC data: n-Alkanes and 1-alkanols. *Fluid Phase Equilib.* **2016**, *412*, 9−20.

(38) Nelder, J. A.; Mead, R. A Simplex Method for Function Minimization. *Comput. J.* **1965**, *7*, 308−313.

(39) Ferrarini, F.; Flôres, G. B.; Muniz, A. R.; de Soares, R. P. An open and extensible sigma-profile database for COSMO-based models. *AIChE J.* **2018**, *64*, 3443−3455.

(40) Gerber, R. P.; Soares, R. D. P. Prediction of Infinite-Dilution Activity Coefficients Using UNIFAC and COSMO-SAC Variants. *Ind. Eng. Chem. Res.* **2010**, *49*, 7488−7496.

DOI: 10.1021/acs.iecr.9b02190
Ind. Eng. Chem. Res. 2019, 58, 16934−16944

(41) Horstmann, S.; Jabłoniec, A.; Krafczyk, J.; Fischer, K.; Gmehling, J. PSRK group contribution equation of state: comprehensive revision and extension IV, including critical constants and α-function parameters for 1000 components. *Fluid Phase Equilib.* **2005**, *227*, 157−164.
(42) Péneloux, A.; Rauzy, E.; Fréze, R. A consistent correction for Redlich-Kwong-Soave volumes. *Fluid Phase Equilib.* **1982**, *8*, 7−23.
(43) Gmehling, J. Isothermal Vapor-Liquid Equilibria in Binary Systems Formed by Esters with Alkenes. *J. Chem. Eng. Data* **1983**, *28*, 27−30.
(44) Kurihara, K.; Minoura, T.; Takeda, K.; Kojima, K. Isothermal Vapor-Liquid Equilibria for Methanol + Ethanol + Water, Methanol + Water, and Ethanol + Water. *J. Chem. Eng. Data* **1995**, *40*, 679−684.
(45) Kehiaian, H. V.; Porcedda, S.; Marongiu, B.; Lepori, L.; Matteoli, E. Thermodynamics of binary mixtures containing linear or cyclic alkanones + n-alkanes or + cycloalkanes. *Fluid Phase Equilib.* **1991**, *63*, 231−257.
(46) Nagata, I.; Hayashida, H. Vapor-Liquid Equilibrium Data for the Ternary Systems: Methyl Acetate-2-Propanol-Benzene and Methyl Acetate-Chloroform-Benzene. *J. Chem. Eng. Jpn.* **1970**, *3*, 161−166.
(47) Handa, Y.; Fenby, D.; Jones, D. Vapour pressures of triethylamine + chloroform and of triethylamine + dichloromethane. *J. Chem. Thermodyn.* **1975**, *7*, 337−343.
(48) Hopkins, J. A.; Bhethanabotla, V. R.; Campbell, S. W. Total Pressure Measurements for Chloroform + Acetone + Toluene at 303.15 K. *J. Chem. Eng. Data* **1994**, *39*, 488−492.
(49) Day, C.-Y.; Chang, C. J.; Chen, C.-Y. Phase Equilibrium of Ethanol + CO2 and Acetone + CO2 at Elevated Pressures. *J. Chem. Eng. Data* **1996**, *41*, 839−843.
(50) Kim, C.-H.; Vimalchand, P.; Donohue, M. D. Vapor-liquid equilibria for binary mixtures of carbon dioxide with benzene, toluene and p-xylene. *Fluid Phase Equilib.* **1986**, *31*, 299−311.
(51) Tochigi, K.; Namae, T.; Suga, T.; Matsuda, H.; Kurihara, K.; dos Ramos, M. C.; McCabe, C. Measurement and prediction of high-pressure vapor-liquid equilibria for binary mixtures of carbon dioxide +n-octane, methanol, ethanol, and perfluorohexane. *J. Supercrit. Fluids* **2010**, *55*, 682−689.
(52) Giles, N. F.; Wilson, H. L.; Wilding, W. V. Phase Equilibrium Measurements on Twelve Binary Mixtures. *J. Chem. Eng. Data* **1996**, *41*, 1223−1238.
(53) Noda, K.; Morisue, T.; Ishida, K. Vapor-LiquidA Equilibria for the Benzene-Cyclohexene-Ammonia System. *J. Chem. Eng. Jpn.* **1975**, *8*, 104−108.
(54) Rizvi, S. S. H.; Heidemann, R. A. Vapor-liquid equilibria in the ammonia-water system. *J. Chem. Eng. Data* **1987**, *32*, 183−191.
(55) Kidnay, A.; Miller, R.; Parrish, W.; Hiza, M. Liquid-vapour phase equilibria in the N2CH4 system from 130 to 180 K. *Cryogenics* **1975**, *15*, 531−540.
(56) Nasir, Q.; Sabil, K. M.; Lau, K. Measurement of isothermal (vapor + liquid) equilibria, (VLE) for binary (CH4 + CO2) from T = (240.35 to 293.15) K and CO2 rich synthetic natural gas systems from T = (248.15 to 279.15) K. *J. Nat. Gas Sci. Eng.* **2015**, *27*, 158−167.
(57) Brown, T.; Sloan, E.; Kidnay, A. Vapor-liquid equilibria in the nitrogen + carbon dioxide + ethane system. *Fluid Phase Equilib.* **1989**, *51*, 299−313.
(58) Dingrani, J. G.; Thodos, G. Vapor liquid equilibrium behavior of the ethane−n butane−n hexane system. *Can. J. Chem. Eng.* **1978**, *56*, 616−623.
(59) Reamer, H. H.; Sage, B. H.; Lacey, W. N. Phase Equilibria in Hydrocarbon Systems. Volumetric and Phase Behavior of the Ethane-n-Pentane System. *J. Chem. Eng. Data* **1960**, *5*, 44−50.
(60) Reamer, H. H.; Sage, B. H. Phase Equilibria in Hydrocarbon Systems. Volumetric and Phase Behavior of the Ethane-n-Decane System. *J. Chem. Eng. Data* **1962**, *7*, 161−168.
(61) Smith, L. C.; Weber, J. H. Liquid Phase Enthalpy Values for The Ethane- n -Butane System. *J. Chem. Eng. Data* **1964**, *9*, 349−351.

DOI: 10.1021/acs.iecr.9b02190
Ind. Eng. Chem. Res. 2019, 58, 16934−16944